Hong et al., http://www.jgp.org/cgi/content/full/jgp.201511483/DC1



### MLCK induces actin bundling but N75 does not

We began our study of the dynamic interactions of MLCK with actin by noncovalently attaching filamentous TRITC-actin to a glass coverslip, followed by biotinylated MLCK and QDs. MLCK consistently induced bundling of the actin. It has been shown previously that MLCK can induce actin bundling in solution (Hayakawa et al., 1994; Ye et al., 1997). Fig. S1 (A and B) shows representative images of TRITC-actin and TRITC-actin-Tm filaments, respectively, attached to a glass coverslip. The fields are populated with single actin filaments that were consistently longer in the presence of Tm. After binding some actin to the coverslip surface, 200 nM N75 was added and incubated for 15–30 min. This peptide did not induce bundling (Fig. S1 C), and nor did 200 nM of a similar construct, GST-N75 (Fig. S1 D). In contrast, the addition of 200 nM of full-length MLCK to actin or actin-Tm resulted in significant bundling (Fig. S1, E and F). The presence of Tm gave longer bundled structures. At 50 nM MLCK, bundling was rarely observed under the same conditions as in Fig. S1 (E and F) but it was evident with longer incubation times. These data suggest that the first 75 N-terminal residues of MLCK alone are not sufficient for bundling activity, in agreement with prior work (Hayakawa et al., 1999) showing that the presence of two actin-binding regions, residues 2–114 and 138–213, are necessary and sufficient for bundling activity of MLCK. Our data suggest that residues 176–213 of the second actin-binding site are important for bundling activity.

To quantify the number of actin filaments per bundle, we assumed that the amount of actin was proportional to the total fluorescence signal intensity. Structures on the coverslip (under the conditions shown in Fig. S1 E) were traced and connected with a continuous line 20 pixels wide (using the ImageJ line tool; Fig. S1 G). Regions in between structures were set to an intensity of 0. The first six peaks appeared to be single filaments by eye and were used to calibrate the scale on the right y axis. Other structures were estimated to have regions with two, three, or four filaments per bundle. Higher intensity structures were common but were difficult to analyze. From many similar scans of other images, we estimated that many of the long bundles, which appear to be single structures, have regions of one to four filaments. For example, the bundle in Fig. S1 F (arrows) contained regions of one, two, and three actin filaments.

Videos were taken to study the dynamics of bundling (Videos 1 and 2). Actin was attached to the surface (templating actin) with some free actin remaining in solution. When MLCK was added, bundles formed in solution and on the coverslip. Bundles that formed in solution frequently zippered down to actin filaments or bundle templates. This latter mechanism must be prominent because we observed few bundles without the actin-templating step. To determine the polarity of actin in the bundles, we inspected fluorescently labeled SMM filaments (Haldeman et al., 2014) moving along a single bundle (see Video 3 as example). Myosin filaments moved in opposite directions on the same bundle, suggesting that at least some of the bundles contain filaments oriented in an antiparallel manner. This was consistent with the movement of single fluorescently labeled myosin X molecules on the bundles, where no evidence was found for unidirectional motion. SMM filaments often stopped at points where the bundle appeared to change actin filament number. This was unlike myosin filaments that moved on a single actin filament, where motion was continuous until they reached the ends (Haldeman et al., 2014). Therefore, we conclude that actin in MLCK-induced bundles is oriented in an antiparallel manner.

It was of interest to determine whether MLCK motion was restricted to certain areas of the bundles, and whether motion was different depending on the regional number of actin filaments. The analysis was inconclusive for several reasons, but primarily because many of the dots do not move (see Fig. S1) and the heterogeneity of the actin bundles, so further work is required to address these questions.

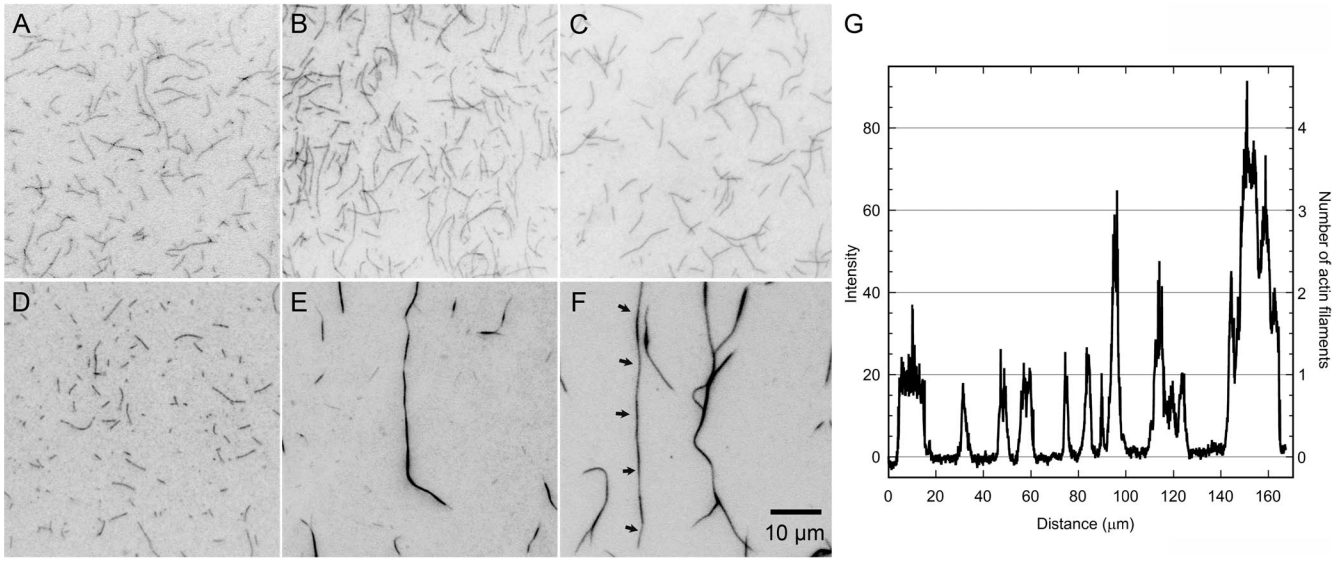


**Figure S1.** Characterization of bundling activity of MLCK and N75 and actin filament number in bundles. (A–F) Wide-field images of TRITC-phalloidin–labeled filamentous actin on a glass surface. (A) 100 nM actin or (B) actin-Tm (molar ratio of 6:1) was applied to a flow cell, and filaments were allowed to attach to the glass coverslip surface for 15 min. After blocking with 2% BSA for 10 min, 200 nM N75 (no GST) (C), GST-N75 (D), or 200 nM MLCK (E) in buffer F was applied to the surface-attached actin and incubated for 15–30 min at 25°C. After washing with actin buffer, imaging actin buffer was applied. (F) The same as E, except with actin-Tm. Arrows in F point to a single bundle that contains regions of one, two, and three actin filaments. All images have the same scale. (G) Calibration of the number of actin filaments per bundle. An image of MLCK-induced actin bundling (image not shown) was found that had six clear single actin filaments (first six peaks in plot) in addition to three bundles (last three peaks). The plot shows the intensity versus distance in a continuous 20-pixel wide line scan connecting these nine unattached actin structures using the line tool in ImageJ. Note that for this scan, the last bundle contained regions with two, three, and four actin filaments.

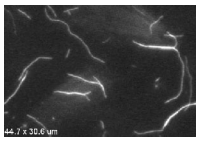

**Video 1.** Dynamics of actin-bundling process induced by MLCK. The following reagents were added in sequence to a glass- or nitrocellulose-coated coverslip: 100 nM of TRITC-labeled F-actin for 10 min (template actin), 5 mg $ml^{-1}$ BSA for 5 min, washed with one flow cell volume of actin buffer, and 200 nM MLCK in actin buffer with oxygen scavengers. All reagents were in actin buffer. Methylcellulose was not included in imaging buffer. The microscope was in TIRF mode set for wide-field excitation at 532 nm with a Hg-Xe lamp, with a 565-nm (TRITC) G-2E\C band-pass emission filter (Nikon), and a 100× objective. At the start of the video, the templating actin is in single filaments with regions of bundling. In the upper center are two hazy areas that are pre-bundled actin just out of the focal plane. Eventually, the more central structures are "captured" by a templated actin filament, and the two structures merge into one large bundle. The one at the top of the image appears to attach to the coverslip directly. Video is 424 × 290 pixels or 44.7 × 30.6 µm, 475 frames at 25 frames/$s^{-1}$, 19 s total. Each pixel is 106 nm.

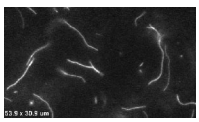

**Video 2.** Dynamics of actin-bundling process induced by MLCK. See Video 1 for methods. Similar to Video 1, with more examples of different stages of the bundling process. Also many single filaments are seen only partially attached to the surface, as indicated by their hazy ends. Video is 511 × 293 pixels or 53.9 × 30.9 µm, 300 frames at 25 frames/$s^{-1}$, 12 s total. Each pixel is 106 nm.

**Video 3.** Example of bidirectional motion of myosin filaments on MLCK-induced actin filament bundles. To determine the polarity of actin bundles, phosphorylated SMM filaments (green; 15) were added to MLCK-induced bundles (red) attached to the surface. Two examples of bidirectional movement are seen on the large hook-shaped bundle (along the direction of the white lines). Note the green filaments moving toward one another, indicating that they must be moving on separate actin filaments with opposite polarity within the bundle. Video is 65 × 128 pixels or 6.8 × 13.5 μm, 321 frames at 25 frames/$s^{-1}$, 12.84 s. Each pixel is 106 nm.

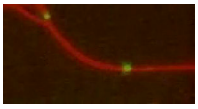

**Video 4.** Example of QD-MLCK molecules moving on an actin bundle. Four MLCK molecules (green) move on actin bundle (red). Video is 132 × 68 pixels or 13.9 × 7.2 μm, 292 frames at 25 frames/$s^{-1}$, 11.68 s total. Each pixel is 106 nm. Condition is imaging buffer D. For all videos, it is recommended that the video be manually sped up to make motion even more obvious to the eye.

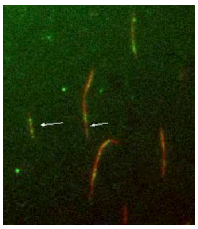

**Video 5.** Example of DyLight-labeled MLCK motion on MLCK-induced actin bundles. MLCK (green) was labeled with DyLight as described in Materials and methods. Note the motion of several MLCKs on actin (red), as was typical. White arrows indicate two areas where single-moving QDs are very evident. The remainder of the field has too many QDs closely spaced to be showing convincing motion, but it does show the extent of colocalization with actin. Note that the image quality is not as good with this small molecule dye compared with QDs. Also, rapid photobleaching of the DyLight probe is evident under these conditions. The observation buffer was imaging buffer E. Video is 252 × 287 pixels or 26.5 × 30.2 μm, 50 frames at 25 frames/$s^{-1}$, 2 s total. Each pixel is 106 nm.

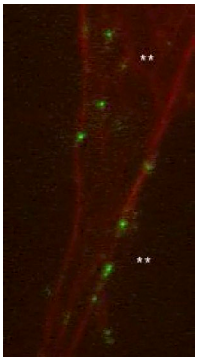

**Video 6.** Example of human biotag-MLCK motion on MLCK-induced actin bundles. Video shows actin in red and QD-MLCK in green. Note the motion of several MLCKs (see white double asterisks), as was typical. The observation buffer was imaging buffer D. Video is 171 × 394 pixels or 18.0 × 41.6 μm, 307 frames at 25 frames/$s^{-1}$, 12.28 s total. Each pixel is 106 nm.

**Video 7.** Example of QD-N75 motion on actin bundles. Video shows actin in red and QD-N75 in green. The observation buffer was imaging buffer D. Video is 121 × 262 pixels or 12.8 × 27.6 µm, 269 frames at 25 frames/$s^{-1}$, 10.76 s total. Each pixel is 106 nm. An arrow points to a moving QD-N75.

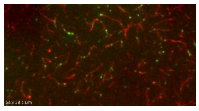

**Video 8.** QD-N75 does not move on single actin filaments. Video shows actin in red and QD-N75 in green. The observation buffer was imaging buffer D. Note that QD-N75 localizes to the actin filaments but does not move on them. Sometimes blinking of closely spaced QDs looks like motion, but it is not. Video is 512 × 270 pixels or 54 × 28.5 µm, 50 frames at 25 frames/$s^{-1}$, 1.6 s total. Each pixel is 106 nm.

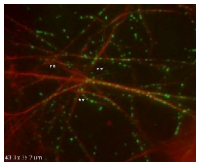

**Video 9.** Example of QD-MLCK moving on HASMC stress fibers. QD-MLCK (green) and stress fibers (red). Video is 411 × 334 pixels or 43.3 × 35.2 µm, 75 frames at 25 frames/$s^{-1}$, 3 s total. Each pixel is 106 nm. The observation buffer was imaging buffer D. Three sets of double asterisks are adjacent to QDs that are clearly moving on actin.

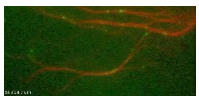

**Video 10.** Another example of QD-MLCK moving on HASMC stress fibers. QD-MLCK (green) and stress fibers (red). Video is 510 × 234 pixels or 53.8 × 24.7 µm, 371 frames at 25 frames/$s^{-1}$, 14.84 s total. Each pixel is 106 nm. The observation buffer was imaging buffer C but at 300 mM KCl (contains ATP). There are many obviously moving single QD-MLCKs. Background green is high caused by freely tumbling molecules entering the TIRF field, because under this condition, the QD-MLCK binds rather weakly to the actin.

## REFERENCES


Haldeman, B.D., R.K. Brizendine, K.C. Facemyer, J.E. Baker, and C.R. Cremo. 2014. The kinetics underlying the velocity of smooth muscle myosin filament sliding on actin filaments in vitro. *J. Biol. Chem.* 289:21055–21070. http://dx.doi.org/10.1074/jbc.M114.564740

Hayakawa, K., T. Okagaki, S. Higashi-Fujime, and K. Kohama. 1994. Bundling of actin filaments by myosin light chain kinase from smooth muscle. *Biochem. Biophys. Res. Commun.* 199:786–791. http://dx.doi.org/10.1006/bbrc.1994.1298

Hayakawa, K., T. Okagaki, L.H. Ye, K. Samizo, S. Higashi-Fujime, T. Takagi, and K. Kohama. 1999. Characterization of the myosin light chain kinase from smooth muscle as an actin-binding protein that assembles actin filaments in vitro. *Biochim. Biophys. Acta.* 1450:12–24.

Ye, L.H., K. Hayakawa, H. Kishi, M. Imamura, A. Nakamura, T. Okagaki, T. Takagi, A. Iwata, T. Tanaka, and K. Kohama. 1997. The structure and function of the actin-binding domain of myosin light chain kinase of smooth muscle. *J. Biol. Chem.* 272:32182–32189. http://dx.doi.org/10.1074/jbc.272.51.32182